

Climatic thresholds shape northern high-latitude fire regimes and imply vulnerability to future climate change

Adam M. Young, Philip E. Higuera, Paul A. Duffy and Feng Sheng Hu

A. M. Young, *Dept of Forest, Rangeland, and Fire Sciences, Univ. of Idaho, Moscow, ID, USA.* – P. E. Higuera (*philip.higuera@umontana.edu*), *Dept of Ecosystem and Conservation Sciences, Univ. of Montana, Missoula, MT, USA.* – P. A. Duffy, *Neptune and Company, Lakewood, CO, USA.* – F. S. Hu, *Dept of Plant Biology, Univ. of Illinois, Urbana, IL, USA, and Dept of Geology, Univ. of Illinois, Urbana, IL, USA.*

Boreal forests and arctic tundra cover 33% of global land area and store an estimated 50% of total soil carbon. Because wildfire is a key driver of terrestrial carbon cycling, increasing fire activity in these ecosystems would likely have global implications. To anticipate potential spatiotemporal variability in fire-regime shifts, we modeled the spatially explicit 30-yr probability of fire occurrence as a function of climate and landscape features (i.e. vegetation and topography) across Alaska. Boosted regression tree (BRT) models captured the spatial distribution of fire across boreal forest and tundra ecoregions (AUC from 0.63–0.78 and Pearson correlations between predicted and observed data from 0.54–0.71), highlighting summer temperature and annual moisture availability as the most influential controls of historical fire regimes. Modeled fire–climate relationships revealed distinct thresholds to fire occurrence, with a nonlinear increase in the probability of fire above an average July temperature of 13.4°C and below an annual moisture availability (i.e. P-PET) of approximately 150 mm. To anticipate potential fire-regime responses to 21st-century climate change, we informed our BRTs with Coupled Model Intercomparison Project Phase 5 climate projections under the RCP 6.0 scenario. Based on these projected climatic changes alone (i.e. not accounting for potential changes in vegetation), our results suggest an increasing probability of wildfire in Alaskan boreal forest and tundra ecosystems, but of varying magnitude across space and throughout the 21st century. Regions with historically low flammability, including tundra and the forest–tundra boundary, are particularly vulnerable to climatically induced changes in fire activity, with up to a fourfold increase in the 30-yr probability of fire occurrence by 2100. Our results underscore the climatic potential for novel fire regimes to develop in these ecosystems, relative to the past 6000–35 000 yr, and spatial variability in the vulnerability of wildfire regimes and associated ecological processes to 21st-century climate change.

Boreal forest and tundra ecosystems cover approximately 33% of Earth's terrestrial surface (McGuire et al. 1995) and are experiencing climatic warming at rates twice as fast as the global average (Serreze and Barry 2011). The ecosystem impacts of warming are well documented, including permafrost thawing (Schuur et al. 2008), shrub expansion (Myers-Smith et al. 2011), altered forest productivity (Beck et al. 2011), and increased fire activity (Kelly et al. 2013). Northern high-latitude ecosystems also play a key role in the global climate system, storing an estimated 50% of global soil carbon (McGuire et al. 2009). The fate of these massive carbon stocks is directly tied to wildfire (Bond-Lamberty et al. 2007, Kelly et al. 2016), and thus to potential shifts in 21st-century fire regimes (i.e. the expected pattern of burning over broad spatiotemporal scales; Baker 2009). For example, the 2007 Anaktuvuk River Fire in the Brooks Foothills ecoregion of Alaska, an event locally unprecedented in the past 6500 yr (Chipman et al. 2015), resulted in an estimated 2.1 Tg C emitted to the atmosphere, comparable to the annual net carbon sink of the tundra biome (Mack et al. 2011). Thus, increased fire activity in this tundra region

would likely result in novel levels of burning, with important implications for ecosystem structure and function, including carbon storage.

Climate warming is expected to alter fire activity globally (Flannigan et al. 2009), but anticipating regional fire-regime shifts requires understanding how potential changes may manifest across space and time. The direction and impacts of shifting fire regimes will vary among ecosystems due to regional variation in climate change, vegetation composition, disturbance histories, ecosystem productivity, and carbon storage. For example, there is a wide range of fire-driven fuel consumption across boreal forests (0.6 to 12.9 kg C m⁻²) due to regional differences in fuel composition and combustion efficiency (van Leeuwen et al. 2014). Therefore, regional differences in fire-regime changes could have important implications for wildfire emissions and carbon cycling. Spatial variability of northern high-latitude fire regimes (Rocha et al. 2012, Boulanger et al. 2013) is ultimately a product of climate and landscape controls on fuel productivity and fuel drying (Kasischke et al. 2010, Parisien et al. 2011). Anticipating potential fire-regime shifts

and associated impacts of 21st-century climate change thus requires understanding the controls of spatial variability in historical fire regimes.

Statistical models of fire–climate relationships at annual timescales across broad regions of boreal forest or tundra suggest strong links between annual area burned and summer moisture deficits, highlighting mechanisms related to low fuel moisture (Duffy et al. 2005, Hu et al. 2015). Consequently, under future scenarios with higher summer moisture deficits, models project increased annual area burned, in some cases by up to 200% by the end of the 21st century (Balshi et al. 2009, Hu et al. 2015). Annual-scale models also have several important limitations for projecting potential fire-regime shifts. First, annual-scale models generally trade off spatial for temporal resolution, with fire and climate information aggregated over broad spatial regions (Duffy et al. 2005, Hu et al. 2015). These models thereby average across regional or sub-regional variation in climate and landscape features that influence fire activity, masking regional variability in future fire activity. Second, these models are inherently sensitive to inter-annual climatic variability, a feature not well captured in global climate models (Rupp et al. 2013).

Multi-decadal scale statistical modeling offers a complementary approach to annual-scale models, trading off temporal for spatial resolution (Parisien et al. 2014). Using spatially resolved long-term (e.g. 30 yr) climatic averages and local landscape features, multi-decadal scale models explain fire occurrence at spatial resolutions from 1 to 100 km² (Krawchuk et al. 2009, Paritsis et al. 2013). These models help reveal mechanisms that drive spatial variation in modern fire activity (Parisien et al. 2014), and they may provide more robust scenarios of future fire activity because they are less sensitive to uncertainty in projections of inter-annual climatic variability (Moritz et al. 2012). While in many ecosystems annual-scale fire–climate relationships align with multi-decadal scale relationships (i.e. warm, dry conditions facilitate burning at both scales), alignment between these two scales is not ubiquitous. For example, fire activity is low in the warmest and driest biomes of Earth, due to consistently high fuel moisture or limited burnable biomass, respectively (Krawchuk and Moritz 2011). It remains unclear where tundra ecosystems fall along this ‘resource gradient’ of burnable biomass. Global-scale analyses suggest that tundra fire regimes may be primarily fuel limited (Moritz et al. 2012), making them fundamentally different from fire regimes in North American boreal forests. This contrasts with evidence from Alaskan tundra, which occupies some of the warmest, wettest regions of circumpolar tundra (Hu et al. 2015) and in some areas has burned as often as boreal forests (Higuera et al. 2011a).

Here we use multi-decadal scale statistical modeling to elucidate the historical drivers of regional fire-regime variability in boreal forest and tundra ecosystems, and then project potential fire-regime changes under 21st-century climate. To quantify historical and future fire regimes, we modeled the spatially explicit 30-yr probability of fire occurrence in Alaska at 2-km resolution using explanatory variables representing climate, vegetation, and topography. The 30-yr probability of fire occurrence can be related to the annual percent area burned, thus allowing a direct comparison

to other fire-regime metrics from historical and paleo-fire records (e.g. fire frequency, mean fire return interval; Baker 2009, Chipman et al. 2015). Alaska is ideal for studying fire–climate relationships in boreal forest and tundra ecosystems, because estimated fire frequencies span several orders of magnitude, from one fire per 50 yr in areas of boreal forests (Kelly et al. 2013) to less than one fire per 10 000 yr in areas of tundra (Chipman et al. 2015). Alaska also offers one of the longest, most continuous fire records available for both boreal forest and tundra (<<http://fire.ak.blm.gov/>>), with high-resolution downscaled climate data available for the region (Scenarios Network for Alaska and Arctic Planning 2015a, b). We expect multi-decadal climate to be an important control of Alaskan fire regimes, but we also expect the nature of fire–climate relationships to vary between boreal forest and tundra ecosystems across this vast region. Thus, two key questions we address in this work are: 1) what are the key climatic and landscape (e.g. vegetation, topography) factors controlling fire-regime variability in Alaskan boreal forest and tundra ecosystems, and 2) how does vulnerability to climatically induced fire-regime shifts vary across Alaska throughout the 21st century?

Material and methods

Response and explanatory variables

Fire presence–absence maps were constructed by converting fire-perimeter data from the Alaska Interagency Coordination Center (<<http://fire.ak.blm.gov/>>) to a 2-km gridded format, spanning the time period from 1950 through 2009 (Fig. 1a). Fires prior to 1950 were excluded due to higher uncertainty in perimeter estimates (Kasischke et al. 2002). While similar studies (Moritz et al. 2012) used a presence-only approach, a presence/absence approach is justified here, as the fire perimeter data used accurately represents burned and unburned areas (Kasischke et al. 2002). Although small fires are almost certainly missing from this dataset, their omission likely has a negligible influence on our results, as most area burned is from large fires (Strauss et al. 1989, Randerson et al. 2012).

Our spatial domain and the distribution of boreal forest and tundra vegetation (Fig. 1a) was defined using the 30-m resolution National Land Cover Database (NLCD) (Homer et al. 2007, Selkowitz and Stehman 2011) and the Circumpolar Arctic Vegetation Map (CAVM) (Walker et al. 2005). The spatial distribution of Alaskan boreal forest is influenced by climate, topography, and past disturbances. Coniferous taxa (*Picea mariana* and *Picea glauca*) dominate late-successional boreal forests, with deciduous taxa (*Betula*, *Populus*) dominant during early succession. A binary ‘forest’ or ‘non-forest’ classification was obtained by merging the NLCD classes, and then further classifying ‘non-forest’ pixels above 650 m in elevation as alpine tundra using a digital elevation model (USGS 1997). We classified all non-forested, but vegetated, pixels below 650 m in elevation as ‘forest’, as these pixels represent post-fire successional vegetation in boreal forest. This classification resulted in a single vegetation type for boreal forest. Tundra was further classi-

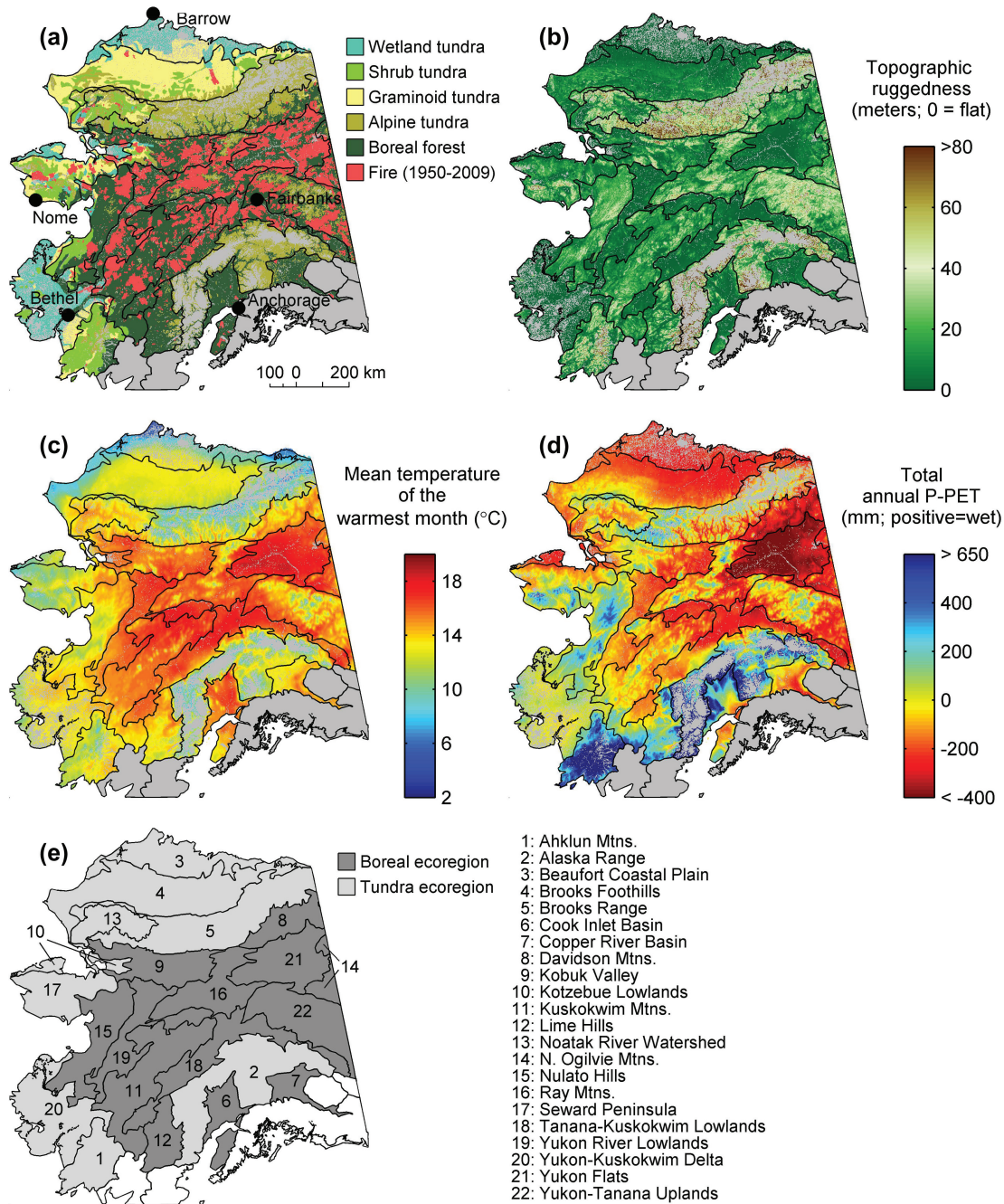


Figure 1. Spatial domain of the study area, including (a) the spatial distribution of vegetation and fire occurrence (1950–2009), (b) topographic ruggedness, (c) 1950–2009 mean temperature of the warmest month (T_{WARM}), (d) 1950–2009 mean total annual moisture availability ($P\text{-}PET_{\text{ANN}}$), and (e) ecoregion classification. Boreal and Tundra classifications of each ecoregion are at the level I stratification, while individual ecoregions are classified at level III. These classifications are slightly modified from those in Nowacki et al. (2001).

fied as graminoid, shrub, wetland, or barrens, by aggregating the 21 CAVM classifications. Graminoid tundra includes tussock tundra (80–100% vegetative cover) and non-tussock tundra (50–100% vegetative cover), which occur in warm and moderately dry regions of the tundra biome, and are dominated by *Carex* and *Eriophorum* (Walker et al. 2005). Shrub tundra includes erect dwarf-shrub (i.e. < 40 cm tall) and low-shrub (i.e. > 40 cm tall) tundra, which occur in warmer, wetter regions relative to graminoid tundra, and are characterized by *Betula*, *Alnus*, and *Salix*. Wetland tundra

occurs on inundated soils, and vegetation can range from graminoid-dominated in cooler regions to shrub-dominated in warmer regions. Barren tundra occurs in cold, dry mountainous regions and is comprised of short-statured, discontinuous vegetation. In our analyses, we reclassified barren tundra as alpine tundra. For boreal forest and tundra, we removed perennial non-burnable areas from the analysis using NLCD classifications of snow/ice, rock, or water. NLCD data were resampled to 2-km resolution using the nearest neighbor procedure.

To account for potential topographic controls on fire occurrence, we constructed a topographic ruggedness (TR) metric (Fig. 1b) (Riley et al. 1999). Topographic ruggedness influences fuel continuity and the density of potential fire breaks on the landscape, and thus regions with more topographic ruggedness likely have a lower probability of burning (Baker 2009). TR was calculated by averaging the absolute difference in elevation between any pixel and its eight surrounding pixels using a 300-m digital elevation model (USGS 1997), which was then resampled using bilinear interpolation to 2-km resolution. TR values closer to zero represent a flatter landscape, while larger TR values represent areas of increased topographic ruggedness.

Climate variables representing energy and moisture availability were selected from 12 candidate variables (Supplementary material Appendix 2, Table A1) constructed from monthly mean temperature and total precipitation data from the climate research unit (CRU) (Harris et al. 2014). These CRU data were statistically downscaled via the ‘delta-change’ method (Fowler et al. 2007) to 2-km resolution using data from the Parameter-elevation Relationships on Independent Slopes Model (PRISM Climate Group, Oregon State Univ., <<http://prism.oregonstate.edu>>) as the baseline map. Downscaling was conducted by and acquired from the Scenarios Network for Alaska and Arctic Planning (2015a). In addition, monthly potential evapotranspiration (PET) was calculated using monthly temperature and Thornthwaite’s PET equation (Thornthwaite 1948; Supplementary material Appendix 2, Table A1). Specifically, we used calculations given in Willmott et al. (1985), which use monthly surface air temperature and day length to estimate total monthly PET for each 2-km pixel. Monthly moisture availability was subsequently calculated by subtracting total monthly PET estimates from the downscaled total monthly precipitation estimates. We performed an initial screening of candidate climate variables, using the Spearman rank correlation between 60-yr averages (1950–2009) of all climate variables (Supplementary material Appendix 2, Table A2). Each variable was then used individually to estimate fire presence and absence for the period spanning 1950–2009. We chose climate variables that had low correlation with each other ($|r_s| \leq 0.5$) and performed best when predicting fire presence and absence, as measured by the area under the receiver operating characteristic curve (see Assessing model performance). This process resulted in the selection of mean temperature of the warmest month (T_{WARM} ; Fig. 1c) and total annual moisture availability (P-PET_{ANN}; Fig. 1d) as our two climatic explanatory variables.

Modeling the probability of fire occurrence

We modeled the presence or absence of fire using boosted regression trees (BRTs) (Elith et al. 2008), implemented with the ‘gbm’ package (Ridgeway 2015) in the R computing environment (ver. 3.2.2, R Core Team). We constructed three sets of models, each comprised of 100 BRTs, which included the entire study domain (‘AK’; i.e. both boreal forest and tundra vegetation), only boreal forest (‘BOREAL’), and only tundra (‘TUNDRA’). Stratifying by these domains allowed us to directly compare fire–climate relationships between

boreal forest and tundra, and evaluate the relative influence of boreal forest and tundra vegetation when included in the AK model. We used a modified version of the Alaskan ecoregions map (levels I and III; Fig. 1e) by Nowacki et al. (2001) to define the spatial domains for each set of models. The primary modification was the addition of the Noatak River Watershed at the level III stratification, defined using the Noatak National Preserve perimeter. Details on the meta-parameters used to fit BRTs and model diagnostics are provided as supplementary information (Supplementary material Appendix 1 and Appendix 2, Fig. A1).

To guard against overfitting of historical fire–climate relationships and account for spatial autocorrelation among 2-km pixels, we developed models using only a randomly sampled subset of 2-km pixels from each spatial domain. Specifically, we conducted a sensitivity analysis that evaluated the tradeoff between varying sampling rates and model performance, with sampling rates determined as a function of the fire-size distribution within each sampling domain (Supplementary material Appendix 1 and Appendix 2, Table A3). Based on this analysis, we used sampling rates that correspond to randomly selecting a single 2-km pixel every 114 km², 122 km², and 74 km², for the AK, BOREAL, and TUNDRA domains, respectively, areas equivalent to the 85th percentile of the fire-size distribution in each domain.

Training datasets were constructed for BRTs using a randomly selected set of 30 (non-continuous) years of paired fire and climate data, and the remaining set of 30 yr was designated as a testing dataset. This partitioning ensured distinct training and testing datasets, to help assess each model’s predictive power. Thirty year time periods are also common for expressing climatological normals, making our results consistent with the context of other global change studies. This 30-yr randomization was done for each of the 100 BRTs.

Assessing model performance

To assess model performance, we used the area under the receiver operating characteristic curve (AUC), commission error rates, and observed vs predicted fire rotation period estimates. AUC values indicate how well BRTs discriminate between observed fire presence and absence in the testing dataset, with 0.5 suggesting no predictive power and 1.0 indicating perfect accuracy. To evaluate how well BRTs captured the potential distribution of fire occurrence, we used a threshold, derived by maximizing the summation of the true positive and true negative rates to calculate commission error rates (Jimenez-Valverde 2012). To assess how well predicted probabilities characterized fire regimes, we compared predicted and observed fire rotation periods (FRPs). The FRP (Eq. 1) is defined as the amount of time it takes to burn an area equal in size to an area of interest

$$FRP = \frac{t}{\left(\sum_{i=1}^n a_i / A \right)} \quad (1)$$

where t is the number of years of observed fire data, a_i is the area burned of each i th of n fires during this time period,

and A is the size of the area of interest (Baker 2009). Within each Alaskan ecoregion (i.e. our areas of interest, Fig. 1e) we calculated predicted FRPs by equating probability values with area burned per pixel in 30 yr (Baker 2009). Observed FRPs were calculated from area burned data using the thirty years in the testing dataset, which included re-burning of pixels. To assess goodness of fit, we calculated Pearson correlation coefficients for each of the 100 BRTs for all three models to evaluate the linear relationship between predicted and observed FRPs.

By sampling 30 yr non-continuously, we assume that 30 yr is enough time to accurately characterize Alaskan fire regimes at the spatial scales considered here, and that fire regimes have been stationary from 1950–2009 at 30-yr timescales. We evaluated these assumptions by comparing the distribution of 100 non-continuous, randomly sampled 30-yr FRPs to the 60-yr FRP from 1950–2009 for each ecoregion (Supplementary material Appendix 2, Fig. A2), and by calculating and comparing FRPs for continuous 30-yr periods at a one-year time step from 1950–2009 (Supplementary material Appendix 2, Fig. A3). Our data meet these assumptions, with one important exception. FRPs in the least flammable ecoregions (e.g. Brooks Foothills) were sensitive to the inclusion or exclusion of individual fire events (Supplementary material Appendix 2, Fig. A2). Thus, characterizing fire regimes in these regions at 30–60 yr time periods is more uncertain than in more flammable regions.

Historical fire-regime controls

We characterized the controls of boreal forest and tundra fire regimes using relative influence values and partial dependence plots. The relative influence of explanatory variables was calculated by summing the number of times a variable was chosen in a BRT, weighted by the BRT improvement of each partition (Elith et al. 2008). The sample mean and standard deviation of the relative influence values from the 100 BRTs were plotted for comparison and visually assessed. Partial dependence plots capture the marginal relationship(s) among response and explanatory variable(s) (i.e. integrating out the influence of other explanatory variables) (Friedman 2001). Partial dependence plots from preliminary analyses revealed nonlinear fire–climate relationships, suggesting climatic thresholds to fire occurrence. To quantify potential thresholds we used a piecewise linear regression (Supplementary material Appendix 1).

Projecting 21st-century fire regimes

We compared historical and future projections of the probability of fire occurrence to understand potential fire regimes under projected climate changes. We used downscaled (2 km) 21st-century projections from five global climate models (GCMs) from the Coupled Model Intercomparison Project Phase 5, provided by the Scenarios Network for Alaska and Arctic Planning (2015b), under the Representative Concentration Pathway 6.0 scenario (CCSM4, GFDL-CM3, GISS-E2-R, IPSL-CM5A-LR, and MRI-CGCM3). These specific models were selected because they were evaluated as

most skillful for Alaska, based on methods from Walsh et al. (2008). We informed our models with 30-yr averages of T_{WARM} and $P\text{-PET}_{\text{ANN}}$ for 2010–2039, 2040–2069, 2070–2099 for each 2-km pixel under each GCM. Our BRTs were then driven with 30-yr climatological normals, while keeping our topographic and vegetation variables unchanged.

To quantify fire-regime responses to future climate change projections, we calculated the fire rotation period for each 2-km pixel using the AK model. To quantify the direction and magnitude of potential fire-regime changes, we present a ratio between projected future fire rotation periods ($\text{FRP}_{\text{Future}}$) and historical fire rotation periods ($\text{FRP}_{\text{Historical}}$), for each pixel (i.e. $\text{FRP}_{\text{Future}}/\text{FRP}_{\text{Historical}}$) (Boulanger et al. 2013). This ratio is < 1.0 if fire activity increases and projected fire rotation periods shorten, and > 1.0 if fire activity decreases and projected fire rotation periods lengthen. For both projected FRPs and the relative change in FRPs, we displayed the median predicted value from all 5 GCMs, as well as projections from the warmest GCM (GFDL-CM3) and the coldest GCM (MRI-CGCM3), defined as T_{WARM} averaged over Alaska from 2010–2099.

Data available from the Dryad Digital Repository: <http://dx.doi.org/10.5061/dryad.r217r> (Young et al. 2016).

Results

Model evaluation

All models adequately discriminated between burned and unburned areas using climate and landscape data, with mean (SD) AUC values of 0.78 (0.02), 0.63 (0.03), and 0.73 (0.06) in the AK, BOREAL, and TUNDRA models, respectively. AK and BOREAL models had low commission error rates, 14% for AK and 20% for BOREAL models, indicating an ability to identify the spatial distribution of fire in Alaska. TUNDRA models were the least accurate in identifying the spatial distribution of fire, with the highest commission error rates (34%) and the highest variability in commission error rates (SD of 18%, compared to 4% for AK and 8% for BOREAL models). Predicted probabilities of fire occurrence captured the spatial distribution of area burned across Alaska (Fig. 2b, c, and d). Median Pearson correlation coefficients ranged from 0.54 in BOREAL models to 0.71 in AK (Fig. 2e, f, and g), indicating overall robust linear relationships between predicted and observed fire rotation periods. Despite the general goodness of fit, models over-predicted the probability of fire occurrence in less flammable ecoregions (Fig. 2e).

Historical fire-regime controls

Temperature of the warmest month (T_{WARM}) and annual moisture availability ($P\text{-PET}_{\text{ANN}}$) had the highest relative influence in all three models, although the magnitude varied among models (Fig. 3). For example, $P\text{-PET}_{\text{ANN}}$ was more important in the BOREAL model than in the TUNDRA model. Topographic ruggedness (TR) had low to moderate influence in all three models, and

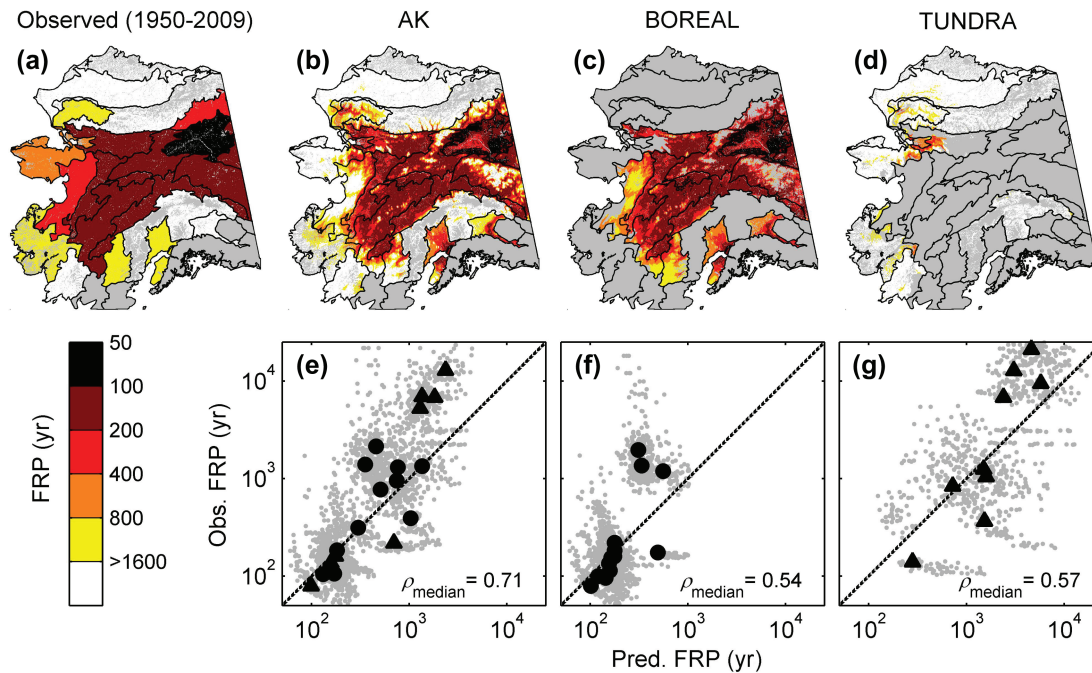


Figure 2. Depictions of model performance, including (a) observed fire rotation periods (FRPs) from 1950–2009 for Alaskan ecoregions as a reference, (b–d) model predicted fire rotation periods for each 2×2 km pixel in Alaska, and (e–g) plots comparing observed fire rotation periods against model predictions per ecoregion. Grey colored points in panels (e–g) are individual predictions and observations from the 100 boosted regression tree models (BRTs), while the filled darker colored circles and triangles are the median predicted and observed FRPs from the 100 BRTs for boreal and tundra ecoregions, respectively. Pearson correlation coefficients (ρ_{median}) are the median recorded Pearson correlation coefficient from a distribution of 100 Pearson correlations comparing the linear relationship between predicted and observed FRPs for each BRT. The x- and y-axes in panels (e–g) are on the \log_e scale. Correlations were calculated on untransformed data.

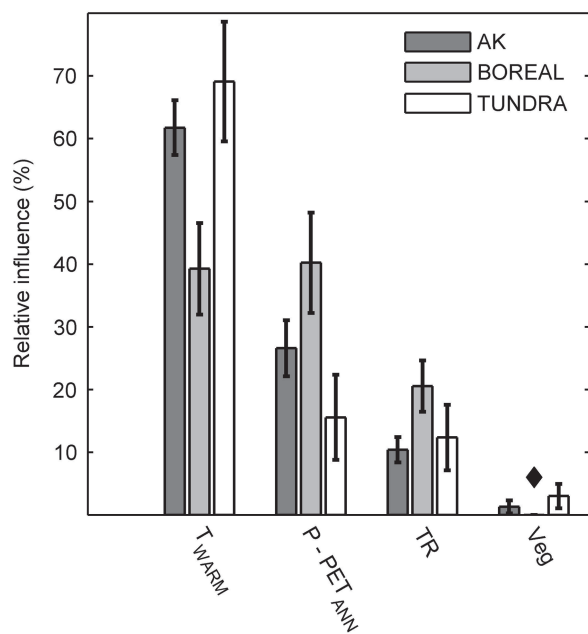


Figure 3. Relative influence of explanatory variables for the Alaska (AK), boreal forest (BOREAL), and tundra (TUNDRA) models. Bar heights represent the sample means and error bars represent ± 1 standard deviation from 100 boosted regression tree models. For the BOREAL model, the relative influence of vegetation (Veg) is 0 by default, as the BOREAL vegetation model has only one class (indicated by the black diamond).

vegetation type had the lowest relative influence in both the AK and TUNDRA models (and was 0 by definition in the BOREAL model).

All three models featured a nonlinear, positive relationship between T_{WARM} and the 30-yr probability of fire occurrence (Fig. 4a, c, e). In addition, the 30-yr probability of fire occurrence was negatively related to $P\text{-}PET_{\text{ANN}}$ in the AK and BOREAL models (Fig. 4b, d). In the TUNDRA model, the relationship between $P\text{-}PET_{\text{ANN}}$ and fire occurrence was non-monotonic, with the wettest and driest regions exhibiting the lowest predicted probabilities compared to regions of moderate moisture availability (Fig. 4f). Interactions between T_{WARM} and $P\text{-}PET_{\text{ANN}}$ were apparent in all three models (Fig. 5a, b, and c), highlighting fire-conducive conditions in warm and dry climates. The relationship between TR and the probability of fire occurrence was non-monotonic for the AK and BOREAL models, with the flattest and most rugged areas exhibiting low probabilities of fire relative to regions with moderate topographic relief (Supplementary material Appendix 2, Fig. A4). In the TUNDRA model, the probability of fire occurrence decreased as TR increased (Supplementary material Appendix 2, Fig. A4).

Segmented regressions analysis revealed temperature (T_{WARM}) and annual moisture availability ($P\text{-}PET_{\text{ANN}}$) thresholds to fire occurrence that were generally similar among all three models. From the bootstrapped samples the average (95% CI) threshold for T_{WARM} was 13.36°C (13.29–

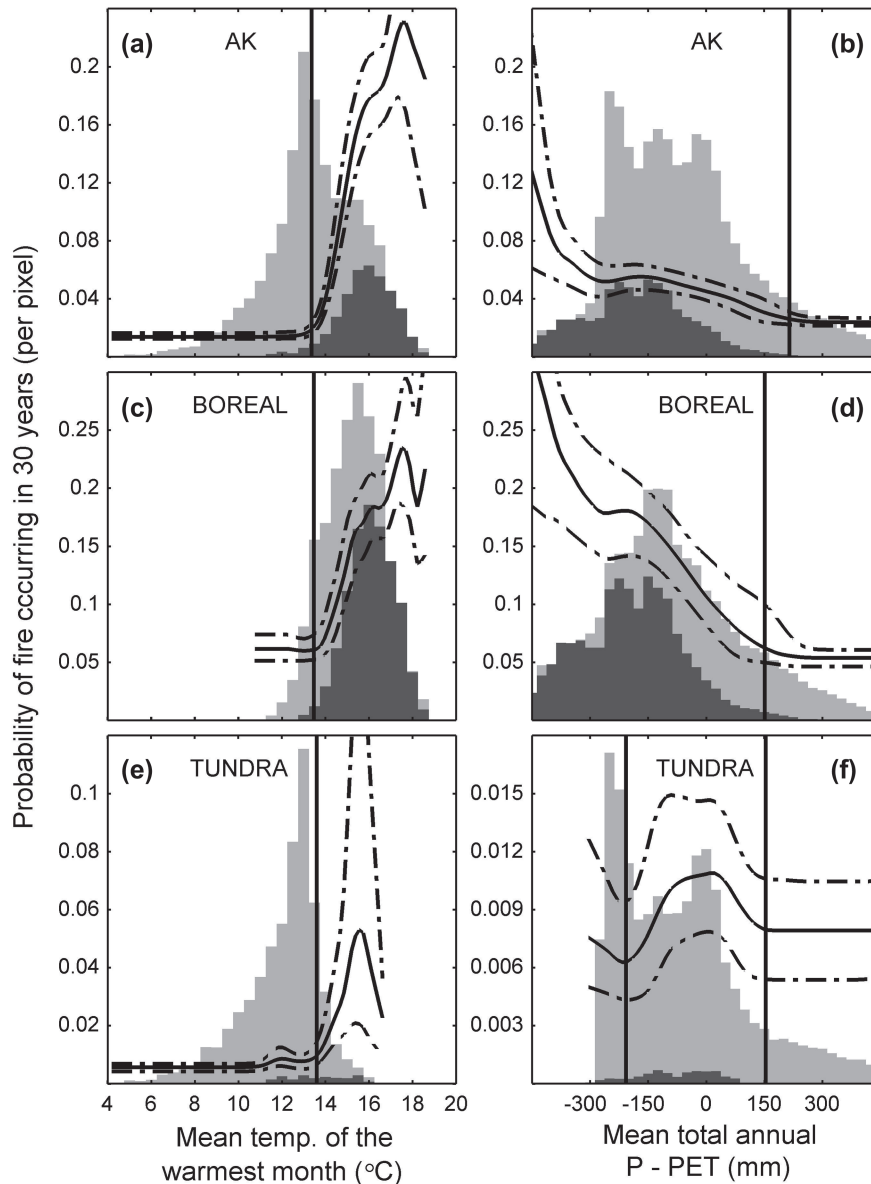


Figure 4. Partial dependence plots illustrating the relationships between the most important explanatory variables and the 30-yr predicted probability of fire occurrence. Rows separate different models, with the Alaska (AK), boreal forest (BOREAL), and tundra (TUNDRA) models displayed from top to bottom. The solid black lines represent the median predicted probability of fire occurrence, and the dashed lines represent the interquartile range from 100 boosted regression tree models. Probability values (y-axis) are presented only for the range of climate conditions (x-axis) observed from 1950–2009. A loess function (span = 0.1) was used to smooth the plotted predicted median and interquartile lines. Vertical lines highlight thresholds, identified as the mean breakpoint from the segmented regression analysis. As a reference, lighter (darker) colored histograms represent the historical distribution of each climate variable among unburned (burned) pixels from 1950 to 2009. Histograms heights were scaled individually and are not associated with y-axis values.

13.45), 13.5°C (13.4–13.6), and 13.65°C (13.50–13.83), for the AK, BOREAL, and TUNDRA models, respectively (Fig. 4a, c, and e). For $P-PET_{ANN}$ threshold estimates averaged 215 mm (40–255) and 151 mm (79–223) for the AK and BOREAL models, respectively, and –207 mm (–225 to –187) and 153 mm (124–182) for the TUNDRA model.

Projected 21st-century changes in climate and fire regimes

The average projected climate change among all five GCMs under RCP 6.0 suggests increases in summer temperature

(T_{WARM}) across all ecoregions, ranging from 0.73–1.19°C during 2010–2039, to 2.33–3.08°C by 2070–2099 (Supplementary material Appendix 2, Fig. A5). Projected annual moisture availability ($P-PET_{ANN}$) exhibits much more spatial variability compared to T_{WARM} for the 21st-century (Supplementary material Appendix 2, Fig. A6). For example, in the Cook Inlet Basin the average projected $P-PET_{ANN}$ for the 2010–2039 period increases by 80 mm relative to the historical period (1950–2009). Comparatively, the Yukon River Lowlands is projected to experience approximately a 60 mm decrease in $P-PET_{ANN}$ during this same time period.

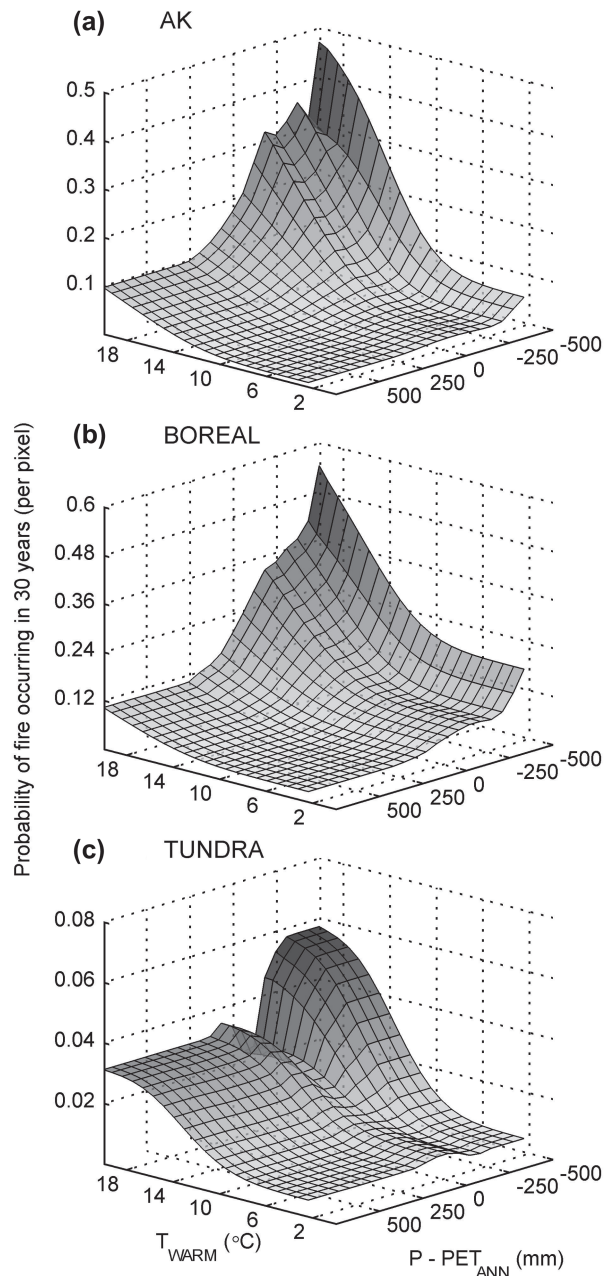


Figure 5. Interactions between the mean temperature of the warmest month (T_{WARM}) and annual moisture availability ($P - \text{PET}_{\text{ANN}}$), and the 30-yr probability of fire occurrence per pixel for the (a) AK, (b) BOREAL, and (c) TUNDRA models. The response surface represents the median predicted probability of fire occurrence from 100 boosted regression tree models for each model type. Darker (lighter) colors in the response surface represent higher (lower) probabilities of fire occurrence. A loess function (span = 0.1) was used to smooth the response surface.

Using the median probability of fire value from among the five GCMs, the AK model predicts shorter fire rotation periods (i.e. more frequent burning) (Fig. 6) in 87, 93, and 97% of our study region for 2010–2039, 2040–2069, and 2070–2099, respectively (Fig. 7). In 43% of our study area, the probability of burning is projected to more than double by mid-century, resulting in fire rotation periods less than half of that predicted for the historical period. In contrast,

13% of our study region is projected to have no change or reduced fire activity for 2010–2039, primarily in boreal forest regions (Fig. 7).

In regions projected to experience an increase in the probability of fire occurrence, the magnitude of change was variable across space and time (Fig. 7). The largest relative increases occur in tundra regions and the cooler boreal forest regions. In regions such as the Brooks Foothills, Yukon-Kuskokwim Delta, or Nulato Hills, fire rotation periods are projected to decrease from greater than 800 to less than 200 yr by the end of the 21st century. In boreal forest the relative magnitude of change is smaller than in tundra and forest–tundra regions, but across most of the boreal forest fire rotation periods are projected to decrease to less than 100 yr by end of the 21st century (Fig. 6).

Discussion

Historical drivers of northern high-latitude fire regimes at multi-decadal timescales

Our study elucidates varying regional vulnerability to climatically induced fire-regime shifts under future climate change. This variability reflects fire–climate relationships shaped by thresholds to fire occurrence, and important interactions between temperature and moisture. Our results indicate that regions characterized by warmer and drier climates support both burnable biomass and frequent fire-conductive weather conditions necessary for fuel drying, ignition, and fire spread. The importance of summer warmth and moisture availability is consistent with annual-scale models from both boreal forest (Duffy et al. 2005, Balshi et al. 2009) and tundra ecosystems (Hu et al. 2010, 2015), which highlight warmer and drier summer conditions as key determinants of annual flammability. This congruence in the importance of summer climate at annual and multi-decadal timescales suggests that both Alaskan tundra and boreal forest are characterized by climate- rather than fuel-limited fire regimes. The primary difference between boreal and tundra fire-regime controls identified in this study is the lower importance of moisture availability in tundra (Fig. 3). This lower importance may reflect the impacts of permafrost underlying tundra soils, which impedes drainage and results in higher fuel moisture than in boreal forest under similar moisture levels (Eugster et al. 2000).

Interactions between summer warmth and moisture availability at 30-yr timescales also determine fuel loading, thereby explaining low fire activity in drier, yet cooler, regions of tundra (e.g. Brooks Range) (Fig. 4f, 5c). In these cool and dry tundra regions, the low predicted probability of fire occurrence provides the only limited evidence of fuel-limited fire regimes in Alaska; however we note that fire occurrence is quite sparse in these tundra regions. Reduced moisture availability, in combination with cooler temperatures, likely results in lower productivity (Walker et al. 2005) and thus reduced fuel availability (Moritz et al. 2012). Finally, lower fire activity in cool and dry tundra regions could also reflect reduced lightning ignitions, due to limited convection and thunderstorm formation (Pfeiffer et al. 2013). Together, this body of work highlights the nature of climatic controls of

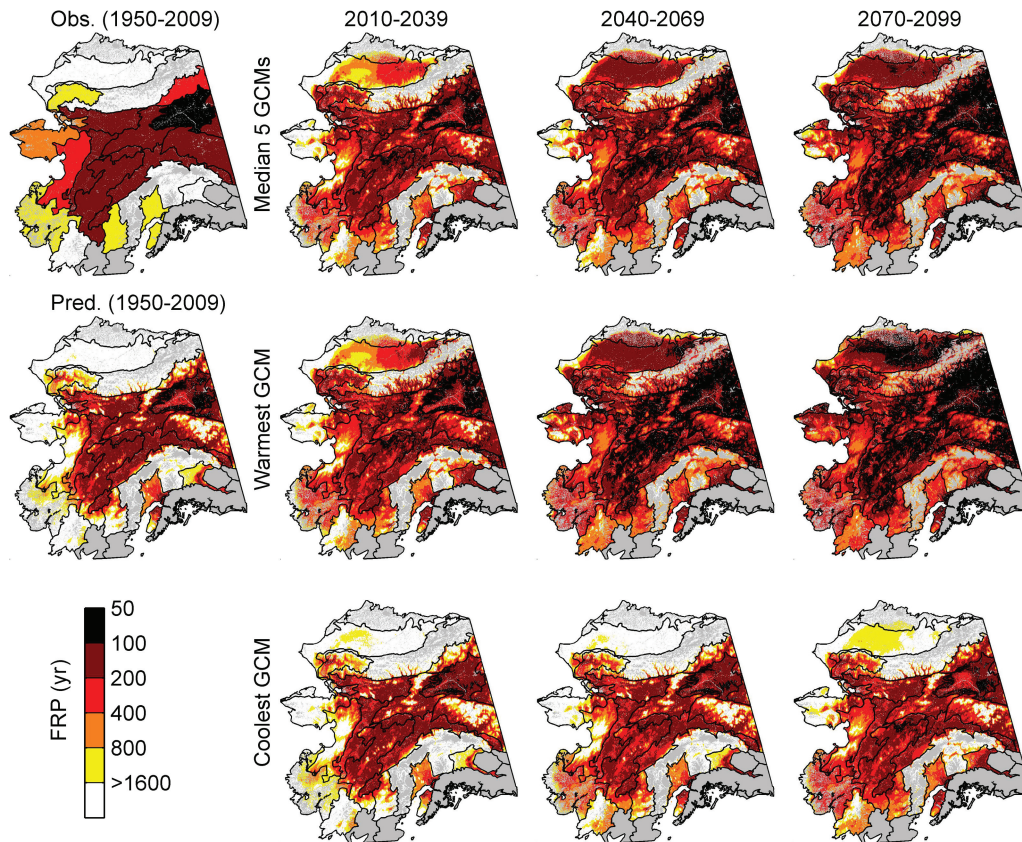


Figure 6. Projected fire rotation periods for three different time periods in the 21st century from the AK model. The left-most column represents historical observed (first row) and predicted (second row) fire rotation periods in Alaska, as a reference.

northern high-latitude fire regimes, from timescales of years to decades, providing key information to anticipate potential fire-regime shifts in the 21st century.

Climatic thresholds drive spatial variability in fire regimes

Fire-climate relationships in boreal forest and tundra ecosystems are characterized by climate thresholds (Fig. 4) that drive regional variation in historical fire regimes. Temperature and moisture thresholds to burning were distinct and consistent across boreal forest and tundra ecosystems, implying that even small shifts in climate could result in large increases or decreases in potential fire activity. Thresholds to burning are also apparent in the Canadian boreal forest at annual (Ali et al. 2012) and multi-decadal timescales (Parisien et al. 2011), and in Alaskan tundra at annual timescales (Hu et al. 2010, 2015). This consistency across timescales suggests links to fundamental mechanisms of wildfire ignition and spread. Specifically, high summer temperatures enhance landscape connectivity of dry fuels, regardless of landcover type, facilitating large fires and thus a high probability of fire occurrence across landscapes (Turner and Romme 1994).

Identification of climatic thresholds to burning also improves our understanding of the climatic drivers of fire-regime changes in historical and paleo-fire records. Increases in fire activity over the past 10–30 yr in Alaska suggest that climatic thresholds to burning are being surpassed,

particularly in regions where climate conditions are near temperature thresholds identified by our models. For example, in boreal forests, ecoregions such as the Davidson Mountains and North Ogilvie Mountains are characterized by July temperatures of 14.2 and 14.4°C, respectively (Supplementary material Appendix 2, Fig. A5), with both regions experiencing large increases in area burned between 2000 and 2010 (Kasischke et al. 2010). Identifying these thresholds also provides context for paleoecological records. For example, Chipman et al. (2015) highlight spatial variability in burning across Alaskan tundra based on paleoecological records spanning the past 6000–35 000 yr. While tundra ecosystems in the south-central Brooks Range experienced frequent burning between ca 14 000 and 10 000 yr ago (Higuera et al. 2008), tundra of the Yukon-Kuskokwim Delta experienced little burning during this same period (Chipman et al. 2015). This contrast likely reflects persistent climatic differences between these regions, with summer temperatures generally above (in the south-central Brooks Range) and below (in the Yukon-Kuskokwim Delta) the approximate 13.4°C threshold.

Vulnerability of northern high-latitude fire regimes to 21st-century climate change

Our modeling results suggest increased fire activity will be widespread across most ecoregions during the 21st century under the RCP 6.0 scenario, equaling or exceeding the

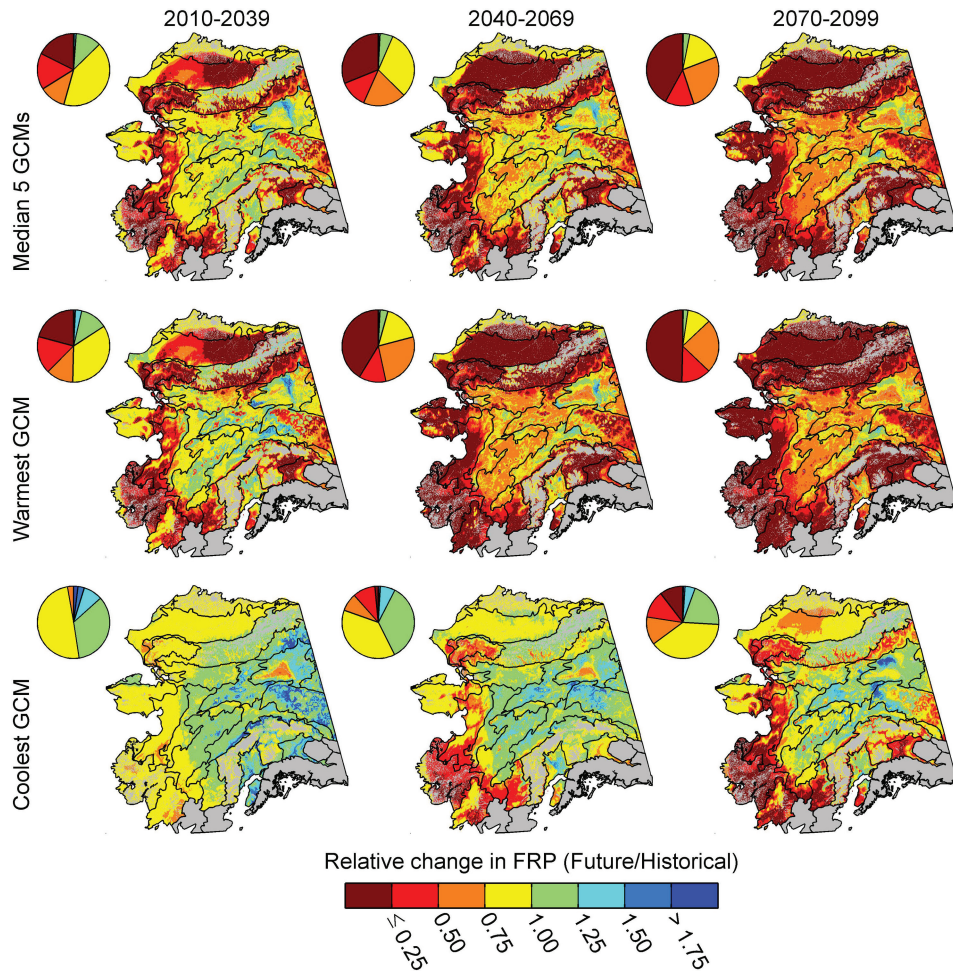


Figure 7. Relative change in the fire rotation period ($FRP_{FUTURE}/FRP_{HISTORICAL}$) per pixel for three different time periods in the 21st century. Change is depicted on a nonlinear scale, where a ratio of 0.5 is equal to a 100% increase in area burned, and a ratio 2.0 is equal to a 50% decrease in area burned. Warmer colors indicate an increase in the future probability of fire and thus decreasing fire rotation periods (i.e. relative difference < 1.0); cooler colors indicate a decrease in the future probability of fire and thus increasing fire rotation periods (i.e. relative difference > 1.0). Pie charts depict the proportions of all pixels in the study domain projected to experience a given level of relative change.

maximum levels of burning inferred from historical and paleoecological records. Across broad regions of Alaskan boreal forests, projected fire rotation periods of 50–100 yr are similar to the highest levels of burning observed during the historical period in the Yukon Flats ecoregion (i.e. since 1950), the most flammable region in Alaska. In some tundra regions (e.g. Brooks Foothills and Yukon-Kuskokwim Delta), projected fire rotation periods of less than 200 yr would be unprecedented in the context of the past 6000–35 000 yr (Higuera et al. 2011b, Chipman et al. 2015). Compared to FRP estimates of 4700 yr for the late Quaternary (Chipman et al. 2015), our models suggest an approximately 20-fold decrease in the FRP in the Brooks Foothills. Although our models overpredict fire activity in low flammability tundra regions during the historical period (Fig. 2e), even a more conservative 5- to 10-fold decrease in the FRP would represent a substantial increase in fire activity.

Projected fire regimes further highlight tundra and cooler boreal forest regions (i.e. the forest–tundra boarder) as the most vulnerable to climatically induced fire-regime shifts, as indicated by the largest changes relative to the historical period (Fig. 7). The vulnerability of these regions is a consequence

of exceeding temperature thresholds to burning (Fig. 4), rather than greater rates of climatic warming compared to boreal forests (Supplementary material Appendix 2, Fig. A5). Forest–tundra regions are also sensitive to other climatically induced ecological changes, including vegetation shifts (Pearson et al. 2013) and permafrost thaw (Schuur et al. 2008). These ecological changes could interact with wildfire to enhance future landscape flammability in tundra and forest–tundra, forming a positive feedback that would accelerate ecosystem shifts, with important implications for northern high-latitude carbon storage. Temperature-induced shrub expansion (Myers-Smith et al. 2011) and drier soils due to permafrost thaw could also serve to increase the probability of fire occurrence (Higuera et al. 2008). In turn, more frequent and potentially repeat burning would likely accelerate permafrost thaw (Rocha and Shaver 2011) and alter vegetation successional trajectories (Jones et al. 2013), further altering soil hydrology and biogeochemical cycling (Mack et al. 2011). The impacts of these potential interactions and feedbacks in tundra and forest–tundra may also be manifested at broader spatial scales, as increased burning (Turetsky et al. 2011), productivity

(Euskirchen et al. 2009), and permafrost thaw (Schuur et al. 2015) all alter soil and ecosystem carbon storage, and thus influence atmospheric greenhouse gas concentrations.

Limitations to anticipating future fire regimes

Our future projections have several important limitations. First, projected climate changes have high uncertainty, due to the dynamics represented in GCMs as well as the scenarios represented by the alternative RCPs (Overland et al. 2014). Second, no-analog climate conditions, relative to 1950–2009, will likely exist in the 21st century. Boosted regression tree models control for extrapolation into these no-analog conditions by ‘clamping down’ on predicted values at the upper and lower limits of each explanatory variable (Elith and Graham 2009), leaving our models constrained and unable to project values of fire activity higher or lower than existed from 1950–2009. Finally, our models do not account for future changes in vegetation, permafrost, or lightning ignitions. Given these constraints, our future projections are best interpreted as indicating the potential location and degree of fire-conducive climatic conditions throughout the 21st century. The inability to represent vegetation changes is particularly limiting, given the known importance of fire–climate–vegetation feedbacks (Higuera et al. 2009, Johnstone et al. 2010, Kelly et al. 2013). The lack of vegetation influence in our models was surprising, but is at least partially an artifact of the categorical nature of our vegetation variables, which are not used as effectively as continuous variables (e.g. T_{WARM}) with our methods. In North American boreal forests, burning can reduce subsequent landscape flammability for years to decades, by causing a shift from more flammable coniferous forests to less flammable deciduous forests (Kelly et al. 2013), or due a reduction in burnable biomass through a shift from landscapes dominated by older to younger forest stands (Héon et al. 2014). Thus, initial climate-induced increases in fire activity during the early 21st century (e.g. Fig. 6) may result in decreased fire activity by mid-century, even if climate becomes more conducive for burning. Conversely, decreased fire activity in the early 21st century may have the opposite effect, as regions with little or decreased burning could serve as ‘fire refugia’, thus helping maintain landscape heterogeneity and flammable coniferous taxa on the landscape (Johnstone et al. 2010).

Despite these limitations, our results highlight the climatic potential for novel fire regimes to develop in tundra and forest–tundra regions by the end of the 21st century, a consequence of climatic thresholds to fire occurrence being surpassed. By quantifying the vulnerability of fire regimes to future climate change, our work helps global change scientists and land managers anticipate the environmental and socioeconomic consequences of climatically mediated fire-regime shifts. Better understanding the potential implications of climatically induced fire-regime shifts will require additional work identifying the mechanisms underlying these 30-yr climatological thresholds to burning at finer spatial scales. How these thresholds interact with non-climatic controls of burning, including ignition variability and human activity, is also a key unknown that will ultimately dictate future fire regimes in northern high-latitude ecosystems.

Acknowledgements – This research and manuscript benefited from discussions with J. Abatzoglou, L. Boschetti, M. Chipman, M. Dietze, R. Kelly, and J. Morris. Funding was provided by NSF grants ARC-1023669 to PEH and PAD, ARC-1023477 to FSH, and a NSF GK12 Fellowship, NASA Earth and Space Science Fellowship NNX14AK86H, and Joint Fire Science Program GRIN Award 14-3-01-7 to AMY. All data and scripts used in this manuscript are publicly available via the Dryad repository (<<http://dx.doi.org/10.5061/dryad.r217r>>), the NSF Arctic Data Center (<<http://dx.doi.org/10.18739/A2MP8P/>>), or upon request to the corresponding author.

References

- Ali, A. A. et al. 2012. Control of the multimillennial wildfire size in boreal North America by spring climatic conditions. – *Proc. Natl Acad. Sci. USA* 109: 20966–20970.
- Baker, W. L. 2009. *Fire ecology in Rocky Mountain landscapes*. – Island Press.
- Balshi, M. S. et al. 2009. Assessing the response of area burned to changing climate in western boreal North America using a multivariate adaptive regression splines (MARS) approach. – *Global Change Biol.* 15: 578–600.
- Beck, P. S. A. et al. 2011. Changes in forest productivity across Alaska consistent with biome shift. – *Ecol. Lett.* 14: 373–379.
- Bond-Lamberty, B. et al. 2007. Fire as the dominant driver of central Canadian boreal forest carbon balance. – *Nature* 450: 89–92.
- Boulanger, Y. et al. 2013. Fire regime zonation under current and future climate over eastern Canada. – *Ecol. Appl.* 23: 904–923.
- Chipman, M. L. et al. 2015. Spatiotemporal patterns of tundra fires: late-Quaternary charcoal records from Alaska. – *Biogeosciences* 12: 4017–4027.
- Duffy, P. A. et al. 2005. Impacts of large-scale atmospheric-ocean variability on Alaskan fire season severity. – *Ecol. Appl.* 15: 1317–1330.
- Elith, J. and Graham, C. H. 2009. Do they? How do they? WHY do they differ? On finding reasons for differing performances of species distribution models. – *Ecography* 32: 66–77.
- Elith, J. et al. 2008. A working guide to boosted regression trees. – *J. Anim. Ecol.* 77: 802–813.
- Eugster, W. et al. 2000. Land-atmosphere energy exchange in Arctic tundra and boreal forest: available data and feedbacks to climate. – *Global Change Biol.* 6: 84–115.
- Euskirchen, E. S. et al. 2009. Changes in vegetation in northern Alaska under scenarios of climate change, 2003–2100: implications for climate feedbacks. – *Ecol. Appl.* 19: 1022–1043.
- Flannigan, M. D. et al. 2009. Implications of changing climate for global wildland fire. – *Int. J. Wildland Fire* 18: 483–507.
- Fowler, H. J. et al. 2007. Linking climate change modelling to impacts studies: recent advances in downscaling techniques for hydrological modelling. – *Int. J. Climatol.* 27: 1547–1578.
- Friedman, J. H. 2001. Greedy function approximation: a gradient boosting machine. – *Ann. Stat.* 29: 1189–1232.
- Harris, I. et al. 2014. Updated high-resolution grids of monthly climatic observations – the CRU TS3.10 dataset. – *Int. J. Climatol.* 34: 623–642.
- Héon, J. et al. 2014. Resistance of the boreal forest to high burn rates. – *Proc. Natl Acad. Sci. USA* 111: 13888–13893.
- Higuera, P. E. et al. 2008. Frequent fires in ancient shrub tundra: implications of paleorecords for arctic environmental change. – *PLoS One* 3: e0001744.
- Higuera, P. E. et al. 2009. Vegetation mediated the impacts of postglacial climate change on fire regimes in the south-central Brooks Range, Alaska. – *Ecol. Monogr.* 79: 201–219.
- Higuera, P. E. et al. 2011a. Variability of tundra fire regimes in Arctic Alaska: millennial scale patterns and ecological implications. – *Ecol. Appl.* 21: 3211–3226.

- Higuera, P. E. et al. 2011b. Tundra fire history over the past 6000 years in the Noatak National Preserve, northwestern Alaska. – *Alaska Park Sci.* 10: 37–41.
- Homer, C. et al. 2007. Completion of the 2001 National Land Cover Database for the conterminous United States. – *Photogramm. Eng. Remote Sens.* 73: 337–341.
- Hu, F. S. et al. 2010. Tundra burning in Alaska: linkages to climatic change and sea-ice retreat. – *J. Geophys. Res. Biogeosci.* 115: G04002.
- Hu, F. S. et al. 2015. Arctic tundra fires: natural variability and responses to climate change. – *Front. Ecol. Environ.* 13: 369–377.
- Jimenez-Valverde, A. 2012. Insights into the area under the receiver operating characteristic curve (AUC) as a discrimination measure in species distribution modelling. – *Global Ecol. Biogeogr.* 21: 498–507.
- Johnstone, J. F. et al. 2010. Fire, climate change, and forest resilience in interior Alaska. – *Can. J. For. Res.* 40: 1302–1312.
- Jones, B. M. et al. 2013. Identification of unrecognized tundra fire events on the north slope of Alaska. – *J. Geophys. Res. Biogeosci.* 118: 1334–1344.
- Kasischke, E. S. et al. 2002. Analysis of the patterns of large fires in the boreal forest region of Alaska. – *Int. J. Wildland Fire* 11: 131–144.
- Kasischke, E. S. et al. 2010. Alaska's changing fire regime – implications for the vulnerability of its boreal forests. – *Can. J. For. Res.* 40: 1313–1324.
- Kelly, R. et al. 2013. Recent burning of boreal forests exceeds fire regime limits of the past 10,000 years. – *Proc. Natl Acad. Sci. USA* 110: 13055–13060.
- Kelly, R. et al. 2016. Palaeodata-informed modelling of large carbon losses from recent burning of boreal forests. – *Nat. Clim. Change* 6: 79–82.
- Krawchuk, M. A. and Moritz, M. A. 2011. Constraints on global fire activity vary across a resource gradient. – *Ecology* 92: 121–132.
- Krawchuk, M. A. et al. 2009. Global pyrogeography: the current and future distribution of wildfire. – *PLoS One* 4: e5102.
- Mack, M. C. et al. 2011. Carbon loss from an unprecedented Arctic tundra wildfire. – *Nature* 475: 489–492.
- McGuire, A. D. et al. 1995. Equilibrium responses of soil carbon to climate change: empirical and process-based estimates. – *J. Biogeogr.* 22: 785–796.
- McGuire, A. D. et al. 2009. Sensitivity of the carbon cycle in the Arctic to climate change. – *Ecol. Monogr.* 79: 523–555.
- Moritz, M. A. et al. 2012. Climate change and disruptions to global fire activity. – *Ecosphere* 3: art49.
- Myers-Smith, I. H. et al. 2011. Shrub expansion in tundra ecosystems: dynamics, impacts and research priorities. – *Environ. Res. Lett.* 6: 045509.
- Nowacki G. et al. 2001. Ecoregions of Alaska. – U.S. Geological Survey Open-File Report 02-297 (map).
- Overland, J. E. et al. 2014. Future Arctic climate changes: adaptation and mitigation time scales. – *Earth's Future* 2: 68–74.
- Parisien, M. A. et al. 2011. Scale-dependent controls on the area burned in the boreal forest of Canada, 1980–2005. – *Ecol. Appl.* 21: 789–805.
- Parisien, M. A. et al. 2014. An analysis of controls on fire activity in boreal Canada: comparing models built with different temporal resolutions. – *Ecol. Appl.* 24: 1341–1356.
- Paritsis, J. et al. 2013. Habitat distribution modeling reveals vegetation flammability and land use as drivers of wildfire in SW Patagonia. – *Ecosphere* 4: art53.
- Pearson, R. G. et al. 2013. Shifts in Arctic vegetation and associated feedbacks under climate change. – *Nat. Clim. Change* 3: 673–677.
- Pfeiffer, M. et al. 2013. A model for global biomass burning in preindustrial time: LPJ-LMfire (v1.0). – *Geosci. Model. Dev.* 6: 643–685.
- Randerson, J. T. et al. 2012. Global burned area and biomass burning emissions from small fires. – *J. Geophys. Res.* 117: G04012.
- Ridgeway, G. with contributions from others 2015. gbm: generalized boosted regression models. – R package ver. 2.1.1, <<http://CRAN.R-project.org/package=gbm>>.
- Riley, S. J. et al. 1999. A terrain ruggedness index that quantifies topographic heterogeneity. – *Intermountain J. Sci.* 5: 23–27.
- Rocha, A. V. and Shaver, G. R. 2011. Postfire energy exchange in arctic tundra: the importance and climatic implications of burn severity. – *Global Change Biol.* 17: 2831–2841.
- Rocha, A. V. et al. 2012. The footprint of Alaskan tundra fires during the past half-century: implications for surface properties and radiative forcing. – *Environ. Res. Lett.* 7: 044039.
- Rupp, D. E. et al. 2013. Evaluation of CMIP5 20th century climate simulations for the Pacific Northwest USA. – *J. Geophys. Res. Atmos.* 118: 10884–10906.
- Scenarios Network for Alaska and Arctic Planning, University of Alaska 2015a. Historical monthly and derived precipitation products – 2 km CRU TS. – <<http://ckan.snap.uaf.edu/dataset/historical-monthly-and-derived-precipitation-products-2km-cru-ts>>, accessed January 2015.
- Scenarios Network for Alaska and Arctic Planning, University of Alaska 2015b. Projected monthly and derived precipitation products – 2 km CMIP5/AR5. – <<http://ckan.snap.uaf.edu/dataset/projected-monthly-and-derived-precipitation-products-2km-cmip5-ar5>>, accessed January 2015.
- Schuur, E. A. G. et al. 2008. Vulnerability of permafrost carbon to climate change: implications for the global carbon cycle. – *Bioscience* 58: 701–714.
- Schuur, E. A. G. et al. 2015. Climate change and the permafrost carbon feedback. – *Nature* 520: 171–179.
- Selkowitz, D. J. and Stehman, S. V. 2011. Thematic accuracy of the National Land Cover Database (NLCD) 2001 land cover for Alaska. – *Remote Sens. Environ.* 115: 1401–1407.
- Serreze, M. C. and Barry, R. G. 2011. Processes and impacts of Arctic amplification: a research synthesis. – *Global Planet. Change* 77: 85–96.
- Strauss, D. et al. 1989. Do one percent of forest fires cause 99-percent of the damage. – *For. Sci.* 35: 319–328.
- Thorntwaite, C. W. 1948. An approach toward a rational classification of climate. – *Geogr. Rev.* 38: 55–94.
- Turetsky, M. R. et al. 2011. Recent acceleration of biomass burning and carbon losses in Alaskan forests and peatlands. – *Nat. Geosci.* 4: 27–31.
- Turner, M. G. and Romme, W. H. 1994. Landscape dynamics in crown fire ecosystems. – *Landscape Ecol.* 9: 59–77.
- USGS 1997. Alaska 300 m digital elevation model. – Anchorage, AK, U.S. Geological Survey – EROS Alaska Field Office, <<http://agdcftp1.wr.usgs.gov/pub/projects/dem/300m/akdem300m.tar.gz>>.
- van Leeuwen, T. T. et al. 2014. Biomass burning fuel consumption rates: a field measurement database. – *Biogeosciences* 11: 7305–7329.
- Walker, D. A. et al. 2005. The circumpolar Arctic vegetation map. – *J. Veg. Sci.* 16: 267–282.
- Walsh, J. E. et al. 2008. Global climate model performance over Alaska and Greenland. – *J. Climatol.* 21: 6156–6174.
- Willmott, C. J. et al. 1985. Climatology of the terrestrial seasonal water cycle. – *J. Climatol.* 5: 589–606.
- Young, A. M. et al. 2016. Data from: Climatic thresholds shape northern high-latitude fire regimes and imply vulnerability to future climate change. – Dryad Digital Repository, <<http://dx.doi.org/10.5061/dryad.r217r>>.

Supplementary material (Appendix ECOG-02205 at <www.ecogeography.org/appendix/ecog-02205>). Appendix 1–2.